Journal of Sedimentary Environments
https://doi.org/10.1007/s43217-024-00202-9

RESEARCH

Depositional facies of the subsurface Neogene Surma Group in the Sangu Gas Field, the Bay of Bengal: records for tidal sedimentation

Shirin Akter[1] · Waheda Akhter[2] · M. Julleh Jalalur Rahman[1] · Md. Sakawat Hossain[1]

Received: 13 February 2024 / Revised: 2 August 2024 / Accepted: 10 August 2024

Abstract
The Neogene Surma Group sandstones are the proven hydrocarbon reservoirs in the Bengal Basin, Bangladesh. This research investigates the depositional facies of the Neogene sequences found in the Sangu-1 and Sangu-5 petroleum exploration wells in the Sangu Gas Field, located in the offshore area of the Bengal Basin, Bangladesh. The Sangu Gas Field, the first offshore gas field, is situated at Block SS 04 in the eastern part of the Hatiya Trough of the Bengal Fore deep and the western extremity of the Chittagong Tripura Fold Belt. This study, utilizing core samples, wireline logs, and seismic data, focused on the depositional characteristics of the Neogene sedimentary rocks. Wireline logs are employed to identify electrofacies patterns, whereas the seismic section is used to differentiate the boundaries of megasequences. The analysis of facies in core samples was conducted based on texture, lithologic association, and internal sedimentary structures. Three distinct facies assemblages were identified, including shale-dominated facies, alternating sandstone and shale assemblages, and sandstone-dominated facies. The presence of various sedimentary structures, such as lenticular, wavy, and flaser bedding, as well as cross-bedded sandstone with mud drapes, indicates evidence of tidal currents. The alternating beds of shales and sandstones observed in cores and well logs are attributed to repetitive transgressive and regressive phases. Overall, the depositional environment of the Neogene Surma Group sequences is interpreted as tide-dominated deltaic. This research will build understanding on the depositional architecture of the potential reservoirs in the offshore Bengal Basin.

Keywords Lithofacies · Electrofacies · Sequences · Depositional environment · Neogene sedimentary rocks · Bay of Bengal

1 Introduction

Prolific hydrocarbon-bearing sedimentary Bengal Basin lies in the north-eastern part of the Indian sub-continent (Fig. 1) and contains approximately ±22 km-thick sedimentary succession of the Cretaceous to Holocene, of which Neogene deposits are more than 6 km. Sedimentation in the Bengal Basin had resulted from the uplift and erosion of the Himalayas and Indo-Burman Ranges (Najman et al., 2022; Uddin & Lundberg, 1998).

Of 31 discovered gas fields in Bangladesh, the Sangu Gas Field, the first offshore gas field, with an initial GIIP (gas initially in place) of 1612 BCF (billion cubic feet) (Cairn Energy, 1998), was discovered in 1996 located at Block SS 04 (Petrobangla, 2016) in the Hatiya Trough (Fig. 1) containing Neogene sandstones and shales of ~18 km (Curray, 1991; Curray & Munasinghe, 1991; Shamsuddin, 2022). Assessment of the depositional environments is required to assess the quality of the reservoir, as it controls the distribution of the petrophysical properties (porosity and permeability) (Greve et al., 2024). Textural properties and facies characteristics are valuable factors in identifying depositional settings (e.g., Irfan et al., 2022; Kanhaiya et al., 2017; Khanam et al., 2022; Singh et al., 2020; Yadav et al., 2023). Depositional facies influence the distribution, volume, architecture, heterogeneity of the reservoir, and ultimately the quality of reservoirs. Few works relating to sedimentology

Communicated by M. V. Alves Martins

✉ M. Julleh Jalalur Rahman
rahman65@juniv.edu

[1] Department of Geological Sciences, Jahangirnagar University, Savar, Dhaka 1342, Bangladesh

[2] Department of Geology, Bangamata Sheikh Fojilatunnesa Mujib Science &Technology University, Jamalpur 2012, Bangladesh

Published online: 19 August 2024

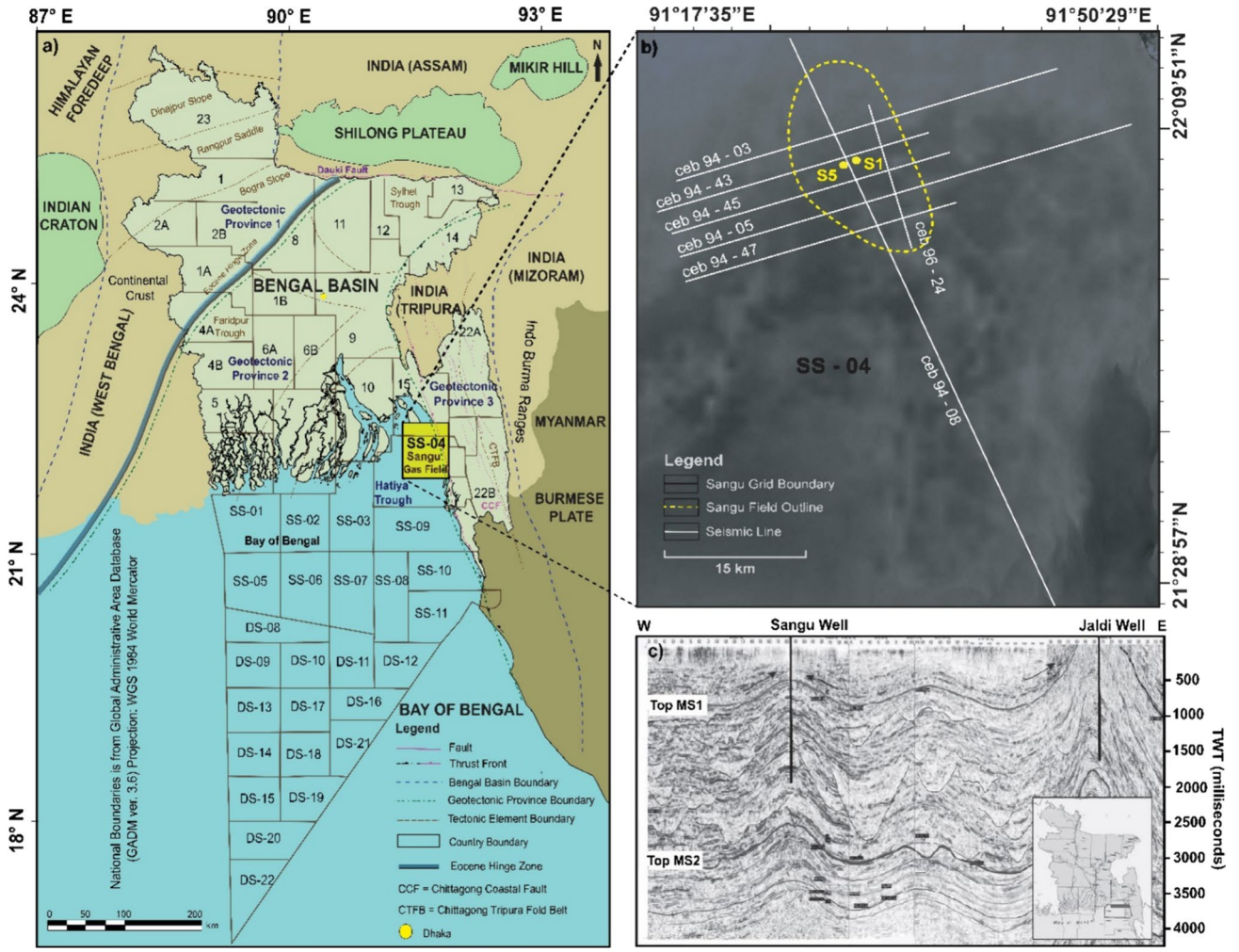

Fig. 1 **a** Potential hydrocarbon block map of offshore Bangladesh with major tectonic division of the Bengal Basin and adjoining areas (Hossain et al., 2019; modified after Petrobangla, 2016) showing the locations of the study region of Sangu Gas Field, **b** location of Sangu-1 and Sangu-5 wells within Block SS-04, and **c** representation of Sangu and adjoining Jaldi structure in Hatiya Trough with seismic character (Modified after Najman et al., 2012)

and diagenesis of Neogene reservoirs of the Sangu Gas Field, Bay of Bengal, and the Hatiya Trough exist (e.g., Matesic, 2012; Najman et al., 2012; Rahman et al., 2022; Shahriar et al., 2020). However, detailed facies analysis of the Neogene sequences in the Offshore Bengal Basin is lacking. Therefore, analyzing detailed facies analysis is important, particularly on the hydrocarbon bearing the Neogene succession in the offshore Bengal Basin to understand the depositional architecture of the potential reservoirs in the offshore Bengal Basin. The main aim of this research work is to infer the depositional environments based on core samples, wireline logs, and seismic sections of the Sangu-1 and Sangu-5 wells.

A detailed description of core samples helps to construct lithofacies, facies association, and facies relationship where different wireline logs are used to delineate electrofacies and, lastly, the boundary of megasequences is defined from the seismic section. Three cores of the reservoir portions of the Sangu-1 well (core-1: 1899–1901 m, core-2: 3010–3012 m, and core-3: 3252–3266 m) and four cores of the Sangu-5 well (core-1: 3498–3501 m, core-2: 3501–3515 m, core-3: 3515–3533 m, and core-4: 3533–3545 m) have been used in this study (Fig. 2).

2 Geologic setting

The Bengal Basin has been divided into three geotectonic provinces of Stable Shelf to the NW, the Foredeep Basin, and the Folded Flank to the east (Fig. 1) based on the regional tectonic setting as well as geophysical investigations, field mapping, and well data (Bakhtine, 1966; Hossain et al., 2020; Reimann, 1993; Shamsuddin & Abdullah, 1997). The southern part of the Foredeep basin is subdivided

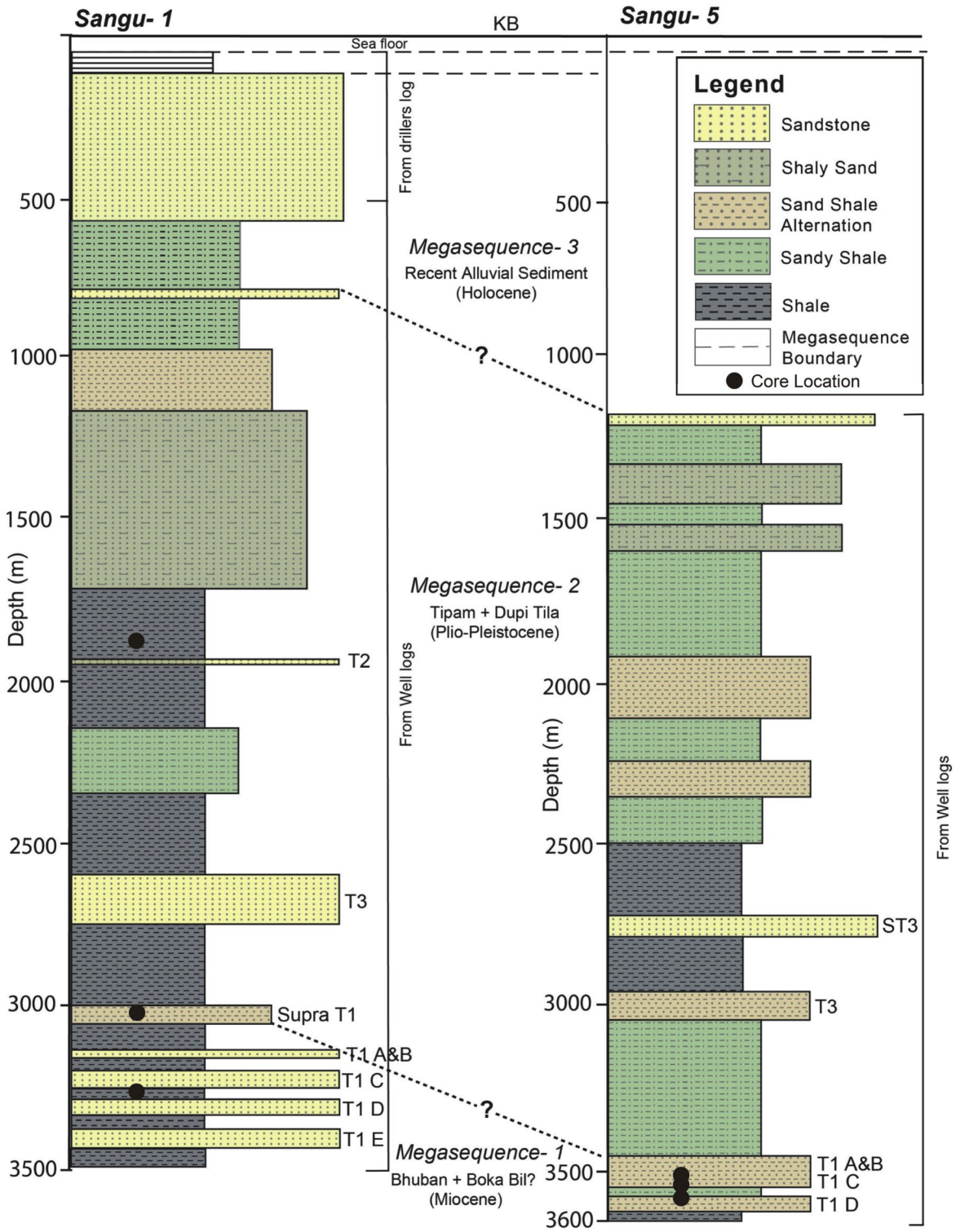

Fig. 2 Lithostratigraphy of the Sangu-1 and Sangu-5 wells (modified after Shahriar et al., 2020). The Neogene succession is divided into megasequences 1, 2, and 3 after Najman et al. (2012). Reservoir names (T3, ST3, T2, T1A, and B, Supra T1, T1C, T1D, and T1E are from Cairn Energy (1998)

into two sub-basins, the Faridpur Trough and the Hatiya Trough, separated by the Barisal-Chandpur High (Guha, 1978). The Sangu Gas Field is located in the Bay of Bengal and lies in the boundary of the Foredeep Basin (Hatiya Trough) and the Chittagong Tripura Fold Belt (CTFB). The foredeep is verged by the frontal folded belt, the CTFB to the east and the continental slope of the Indian Craton to the west (Reimann, 1993) and the basin plunges into the Bay of Bengal beneath the continental shelf (Matin et al., 1986) to the south with an NE–SW general trend. The Hatiya Trough is about 18 km deep depression, extending southward to about 18°N latitude (Curray et al., 1993; Singh et al., 2016) and forming the outermost part of the westward-propagating CTFB. The Sangu structure is an asymmetric anticline (NNW–SSE trending) with a four-way dip covering an area of 10 km × 25 km (Shahriar et al., 2020). Underlined by oceanic crust, the Hatiya Trough and most of the Bengal Foredeep are formed following the break-away of India from Australia and Antarctica during the Early Cretaceous (Curray, 2014; Maurin & Rangin, 2009). Sediments of Late Neogene–Recent time were in general derived from the Himalayan mountain belt (Najman et al., 2016), whereas a minor amount of arc-derived sediments were from the Trans-Himalaya or Paleogene Indo-Burman Ranges (Rahman et al., 2017, 2020; Yang et al., 2019, 2020).

The stratigraphic succession of the South Bengal Basin (Hatiya Trough—deeper part of the Bengal Basin) is of Neogene age starting with the basal Surma Group, which is overlain by the Tipam Formation and Dupi Tila Formation, respectively (Fig. 3). The Surma Group is the result of a major delta progradation since the Early Miocene and is thought to have been characterized by repetitive transgressive and regressive phases that resulted from tectonic subsidence as well as relative sea-level changes (Rahman et al., 2009, 2017). The Middle Miocene Bhuban Formation and the Late Miocene Boka Bil Formation are Miocene sediments that make up the Surma Group's marine-deltaic deposits. Fluvial braided deposits are represented by the younger succession of the Middle Pliocene Tipam Formation, while fluvial meandering deposits are represented by the Late Pliocene–Pleistocene Dupi Tila sandstones.

3 Methods

The depositional architecture of the Neogene Surma Group from the Sangu Gas Field, Bay of Bengal, has been reconstructed through a comprehensive documentation of facies, facies association, and facies relationships in cores. This was achieved by analyzing lithofacies (texture, lithologic association, and internal sedimentary structures) and unit contacts, following Miall's (2010) schemes. An electrofacies approach was developed and applied to identify depositional environmental settings based on gamma ray log trends/patterns, which are sensitive to sand–shale changes in rock formations. The gamma ray log was used as the primary analytical tool to infer paleo-environment, with sedimentological attributes recorded, photographed, and presented in graphical logs. A sequence stratigraphic approach was utilized to divide the rock record into various units (parasequences, parasequence sets, and systems tracts) by identifying bounding discontinuities such as maximum flooding surface, transgressive surface, regressive erosion surface, and incised valley floor. This allowed for the identification of key stratigraphic surfaces and systems tracts, enabling the differentiation of different depositional sequences.

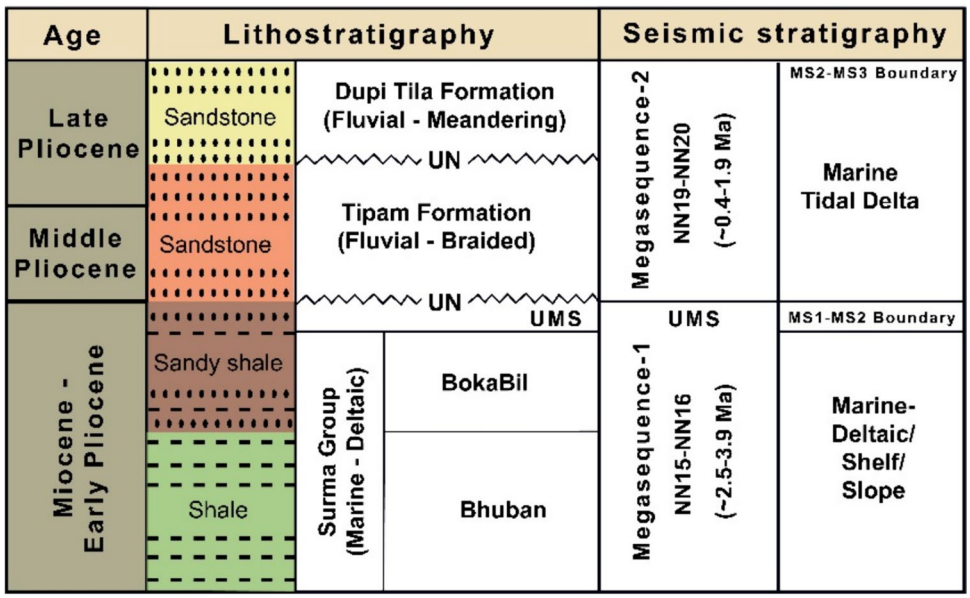

Fig. 3 Stratigraphy of the Southern Bengal Basin (Hatiya Trough). The left-hand panel shows the lithostratigraphy (modified after Uddin & Lundberg, 1998) and the right-hand panel shows the seismic stratigraphy (modified after Najman et al., 2012) (UN—unconformity and UMS—upper marine shale)

4 Facies assemblages and interpretation

4.1 Lithofacies

Facies analysis of core samples from Sangu-1 well (1898–3266 m) and Sangu-5 well (3498–3545 m) was carried out precisely based on texture, lithologic association, and internal sedimentary structures. Three distinct facies assemblages are recognized as shale-dominated facies, Alternating sandstone and shale facies and sandstone-dominated facies (Table 1).

4.1.1 Shale-dominated facies assemblages

Shale-dominated facies assemblages are characterized by sand/slit lenticules and streaks. These are (Fig. 4) mainly bluish gray colored, thin, and evenly laminated and encountered mainly in the Sangu-1 well at depths of 3256.90–3257.00 m and in the Sangu-5 well at depths of 3512.72–3513, 3515.86–3516.09, 3517.12–3517.35, and 3518.91–3519.31 m. Bioturbation (Fig. 4b) is a common feature filled by sand/silt. Vertical burrows are present occasionally and ball and pillow or load structure (Fig. 4d) is present at 3519.65–3520 m depth in Sangu-5 well. Lenticular bedded (L_n) subfacies are bluish gray to light gray color shale with thin lenses (Fig. 4e, f) of fine sand/coarse silt. The lenses are both isolated and occasionally connected with various dimensions. Sometimes, sand/silt streaks and convoluted structure are observed (Fig. 4c). Shale-dominated facies assemblages are deposited as middle to inner shelf deposits in quiet water depositional settings. Current energy is lowest in the upper part of the intertidal zone, which causes the deposition of shale and lenticular shale (muddy sediment), whereas sand/silt streaks have been deposited under high tidal influence and/or storm (Reineck & Singh, 1980).

4.1.2 Alternating sandstone and shale facies

Alternating bluish-gray shale and light gray sandstone are observed in which sand lenses are well connected and laterally comprise wavy bedded sandstone facies (Fig. 4f) and encountered in the Sangu-1 well at a depth of 3011.90–3012.00, and 3255.18–3255.24 m, and in the Sangu-5 well at a depth of 3508.75–3509.00 and 3515–3515.13 m. Sometimes, bioturbation has is observed in both shale and sandstone. Deposition of wavy bedded sandstone occurs in the middle part of the intertidal zone during low to moderate energy conditions.

Table 1 Lithofacies and facies associations documented from core samples of Sangu-1 and Sangu-5 wells

Facies association	Lithofacies	Brief description	Interpretation
Shale-dominated facies	**1a.** Shale (F_m) **1b.** Lenticular bedded shale (L_n)	Bluish gray to dark gray shales, and minor massive mudstone; occasionally faintly bioturbated; shales with lenticles of very fine sand/silt (Fig. 4e), lenticles show small-scale cross-lamination	Upper part of the intertidal zone
Alternating sandstone and shale facies	**2.** Wavy bedded sandstone (S_w)	Alternating straight to slightly wavy bluish-gray shale and very fine-grained light gray sandstones (Fig. 4f)	Middle part of the intertidal zone during low- to moderate-energy conditions
Sandstone-dominated facies	**3a.** Flaser bedded sandstone (S_f) **3b.** Rippled cross-laminated sandstone (S_r)	Very fine-grained to fine-grained; ripples are commonly asymmetrical, bipolar; mud-draped. Shale/mudstone flasers occur on the ripple troughs (Fig. 4g)	Lower intertidal to upper subtidal zone
	4. Parallel-laminated/bedded sandstone (S_h)	Light gray-colored, fine- to medium-grained, horizontal to nearly horizontal upper plain bed lamination (Fig. 5b)	Shallow tidal channel during the upper flow regime
	5. Trough cross-bedded sandstone (S_t) **6.** Planar cross-bedded sandstone (S_p)	Light gray-colored, fine- to medium-grained, planar as well as tangential foresets and mud clasts along foresets (Fig. 5a, c, d)	Mostly subtidal
	7. Massive sandstone (S_m)	Light gray colored, fine to medium grained, sometimes with mud clasts (Fig. 5f)	Channel fill deposits

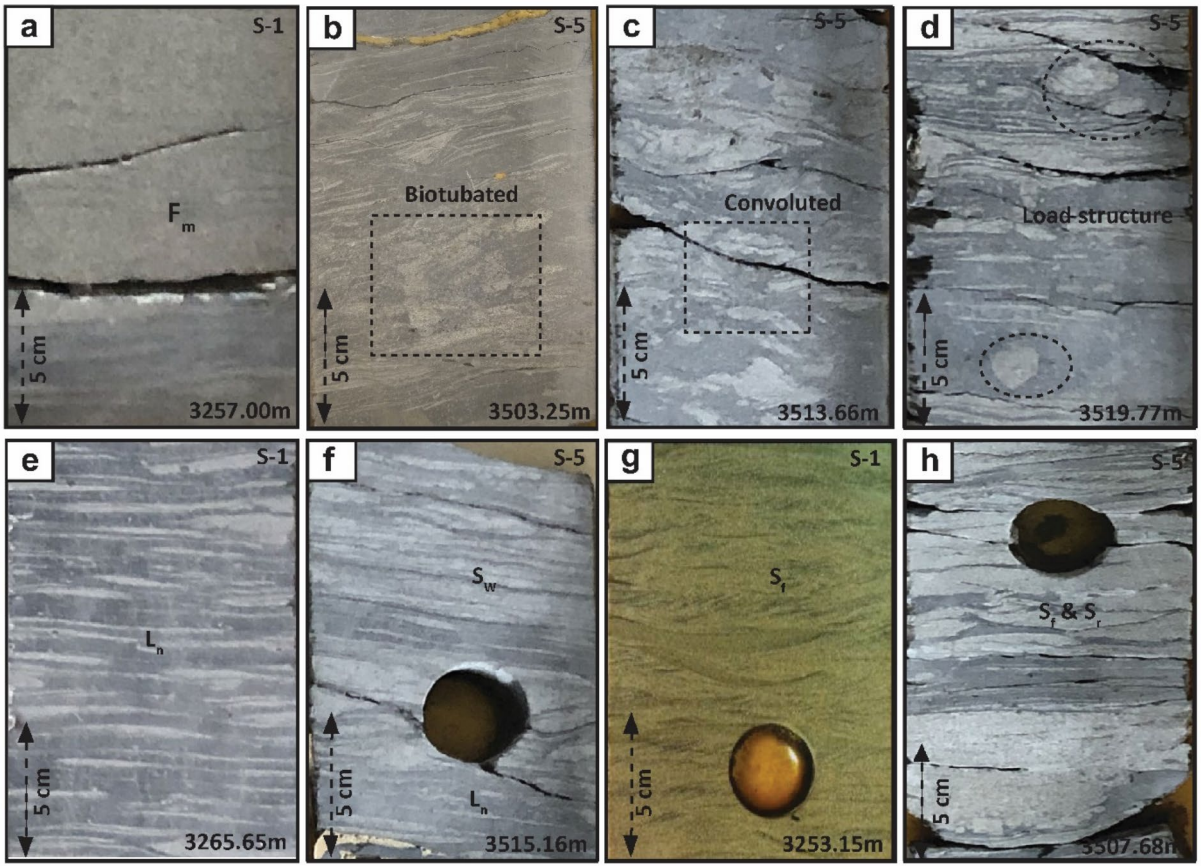

Fig. 4 Sedimentary structures representing shale-dominating facies assemblages and alternating sandstone and shale facies; **a** shale facies at 3256.85 m depth in Sangu-1 well, **b** bioturbated shale at 3503.10 m depth, **c** convoluted shale at 3513.51 m depth, **d** shale with load structure at 3519.60 m depth in the Sangu-5 well, **e** lenticular bedded facies (L_n) at a depth 3265.50 m in the Sangu-1 well, **f** coarsening upward sequence where lenticular bedded facies passing upward into wavy bedded facies at 3515.02 m depth in Sangu-5 well, **g** flaser bedded facies (S_f) at 3253.00 m depth in the Sangu-1 well, and **h** ripple-laminated facies (S_r) and flaser bedded facies (S_f) at 3507.50 m depth in the Sangu-5 well

4.1.3 Sandstone-dominated facies

Sandstone-dominated facies comprises flaser bedded sandstone, parallel-laminated/bedded sandstone (S_h), trough cross-bedded sandstone (S_t), planar cross-bedded sandstone (S_p), and massive sandstone facies (S_m). Flaser bedded sandstone is encountered in the Sangu-1 well at depths of 3011.90–3012.00 and 3255.18–3255.24 m, and in the Sangu-5 well at depths of 3508.75–3509.00, 3515–3515.13 m. Gray to light gray color, fine-grained sandstones are rippled and mud drapes along the foreset laminae and flasers usually occur on the ripple troughs forming flaser bedding (Fig. 4g, h), sometimes continuing on the lower part of the ripple laminae. Parallel-laminated/bedded sandstone facies is characterized by light gray color, fine- to medium-grained sandstone, horizontal to nearly horizontal, and thin beds and typical upper plane bed lamination. Parallel-laminated/ bedded facies (Fig. 5a, b) is encountered in the Sangu-1 well at a depth of 3252.00–3252.25 m, whereas in the Sangu-5 well at a depth of 3528.49–3529.00, and 3543.53–3544 m, etc. Trough cross-bedded sandstone facies (Fig. 5d) is characterized by light gray color, fine- to medium-grained, and curved or tangential upper/lower bounding surface, which is a very familiar facies encountered in the Sangu-5 well at a depth of 3522.00–3522.70, 3531.16–3533.00, and 3542.62–3543.00 m, and in the Sangu-1 well at a depth of 3257.00–3257.22 m. Occasionally, beds are attenuated by thin mud laminae. Planar cross-bedded sandstone facies is characterized by light gray color, fine- to medium-grained, low-angular bedsets with planar upper and lower bounding surfaces (Fig. 5a, c), which is a common facies encountered in the Sangu-1 well at depths of 3252.40–3252.55 and 3256.20–3256.50 m, and in the Sangu-5 well at depths of 3520.00–3520.20, 3521.75–3522.00, and 3525.00–3526.27 m. Light gray-colored, fine- to medium-grained massive sandstone (Fig. 5f) is common in the core-3 encountered in the Sangu-1 well at a depth of 3010.18–3010.23 and 3257.15–3257.23 m,

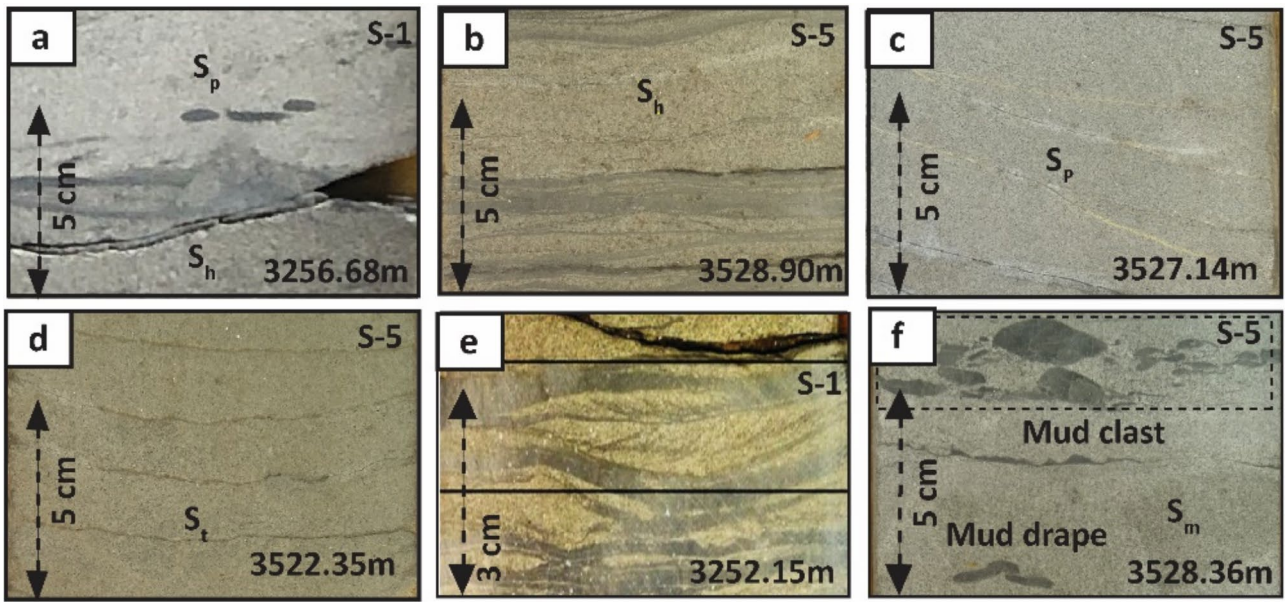

Fig. 5 Sedimentary structures representing sandstone-dominating facies; **a** parallel-laminated sandstone (S_h) facies and low-angle planar cross-bedded sandstone (S_P) facies at 3256.60 m depth in the Sangu-1 well, **b** parallel-laminated sandstone (S_h) facies at 3528.82 m depth, **c** low-angle planar cross-laminated sandstone (S_P) facies at 3526.97 m depth in the Sangu-5 well, **d** trough cross-bedded sandstone facies (S_t) at 3522.27 m depth, **e** herringbone structure at 3252.11 m depth in the Sangu-1 well, and **f** the presence of mud clasts in massive sandstone facies (S_m) at 3528.28 m depth in the Sangu-5 well

and in the Sangu-5 well at a depth of 3520.20–3521 and 3522.70–3523.19 m. Sometimes, mud streaks or clasts are also visible.

Deposition of sandstone-dominated facies occurs by strong traction currents. Flaser bedded sandstones occur in the lower intertidal to upper subtidal zone (De Raaf & Boersma, 1971). Formation of parallel-laminated sandstone is due to high energy condition in the upper flow regime condition in shallow tidal channel, or develop as deposits of high velocity and highly turbulent flows (Rahman et al., 2009) by migrating bed forms on sandy deposits in shallow subtidal environment under the influence of which high tidal energy cross-bedded sandstone facies get deposited (Rahman et al., 2009). Massive sandstone with mud clasts indicates channel-fill deposits.

4.2 Electrofacies

Abrupt changes in the gamma ray (GR) log response are interpreted to be related to sharp lithological breaks associated with unconformities and sequence boundaries (Krassay, 1998) to distinguish different sedimentary environments, as the fining and coarsening upward cycles are often related to changes in grain size and clay contents (Cant, 1992). In the Sangu-1 (500–3420 m) and Sangu-5 wells (1175–3660 m depth), five log facies are discerned, namely funnel-shaped facies, bell-shaped facies, box-car facies, bow-shaped facies, and serrated-shaped facies.

Funnel-shaped facies indicates a coarsening upward or cleaning up facies trend (Fig. 6a). Usually, it forms due to upwardly increasing depositional energy related to delta progradation. This facies is commonly observed at depths of 1150–1200, 3320–3400 m, etc. in the Sangu-1 well and 1335–1520 and 3130–3343 m in the Sangu-5 well. Bell-shaped facies represents fining upward or dirtying up facies trend (Fig. 6b), which indicates a retreating shoreline–shelf system in shallow marine setting, fluvial or deltaic channels (Emery & Myers, 1996; Selley, 1985, 1998) with decreasing depositional energy. It is a very common type of facies found at depths 1185–1220 and 3450–3500 m in the Sangu-1 well and 1600–1800, 2982–3343 and 3450–3575 m in the Sangu-5 well. Box-car-shaped facies is observed at both the left and right. The left box-car facies (Fig. 6e) reflects the tidal aggradational sand bodies deposited in high energy conditions with sharp upper and lower end of low GR value due to erosional bases truncating the underlying shale causing the sharp basal boundary in tide-dominated channel. It is more commonly observed at 1915–2000 and 2247–2369 m depth in the Sangu-5 well than Sangu-1 well. In tidal flats, right box-car facies (Fig. 6d) reflects the aggradational shale having no internal irregularities with abrupt overlying and underlying boundaries and deposits mostly in low energy conditions. It is observed at depths 2500–2790 m in the Sangu-1 well and 2800–2982 and 3356–3450 m in the Sangu-5 well.

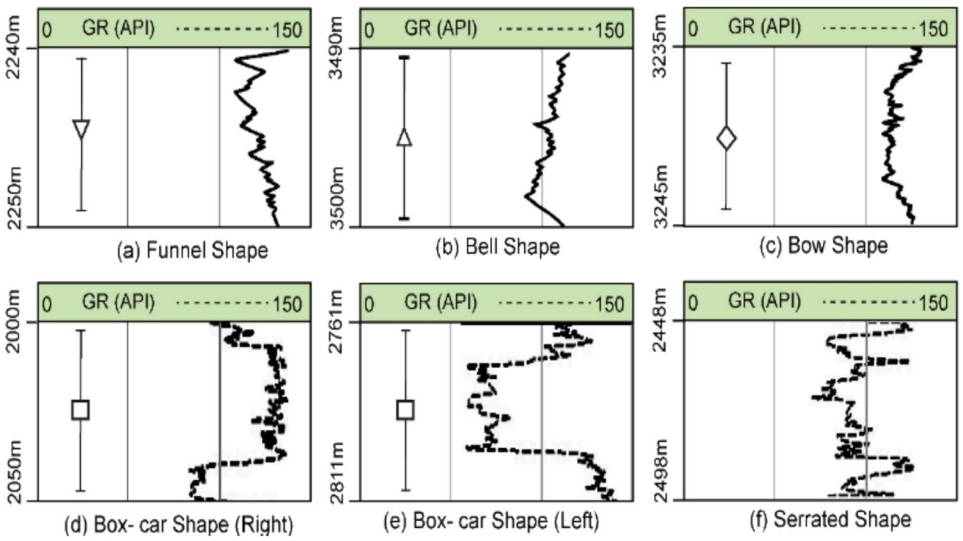

Fig. 6 GR log trends in the Sangu-1 and Sangu-5 wells; **a** funnel shape at 2240 m depth in the Sangu-1 well, **b** bell shape at 3490 m depth in the Sangu-1 well, **c** bow shape at 3235 m depth in the Sangu-1 well, **d** right box-car shape 3350 m depth in the Sangu-5 well, **e** left box-car shape at 2811 m depth in the Sangu-5 well, and **f** serrated shape at 2498 m depth in the Sangu-5 well

Bow or symmetrical trends (Fig. 6c) consist of a coarsening upward trend overlain by a fining upward trend with no significant break (Emery & Myers, 1996). This trend forms in tide-dominated delta (mixed tidal flat) as a result of a waxing and waning of clastic sedimentation rate in a basinal setting such as during the progradation and retrogradation. It is less common in the studied section and observed at 1360–1500 m depth in the Sangu-1 well and 2592–2650 and 3450–3498 m depth in the Sangu-5 well. Fluctuation of GR reading with high and low values with thin laminated sand mud intercalation, having no systematic change in either the sand baseline or shale baseline and lacking the clean character of the box-car trend results in serrated shape or irregular facies (Fig. 6f) (Emery & Myers, 1996). For instance, this trend forms a tide-dominated (muddy tidal flat) environment.

5 Discussion

Precise and detailed depiction of texture, lithologic association, and internal sedimentary structures of the core samples encountered in Sangu-1 and Sangu-5 wells have provided a subtle concept about the depositional environments of the Neogene Surma Group. Alternating beds of shales and sandstones as revealed from cores (Fig. 7) and well logs (Fig. 8) of Sangu-1 and Sangu-5 wells are the result of long-term changes in the hydrodynamic conditions within a sedimentary basin (Singh & Singh, 1995) indicating meso- to macrotidal environments.

The Neogene Surma Group encountered in Sangu-1 and Sangu-5 wells is characterized by lenticular bedding, wavy bedding, flaser bedding, parallel lamination, trough cross-bedded, and planar cross-bedded sedimentary structures (Figs. 4, 5). The presence of mud drapes deposited between high-water and low-water tides indicates tidal environments (De Raaf & Boersma, 1971; Klein, 1971). Tidal influence in inter-tidal depositional setting is indicated by the association of lenticular bedded, wavy bedded and flaser bedded facies representing a fining upward sequence (Ginsburg, 1975; Klein, 1985; Reineck & Wunderlich, 1968).

The presence of bimodality in ripple cross-lamination confirms its tidal influences undisputedly, though these associations are also observed in a number of modern non-tidal environments (De Raaf & Boersma, 1971). Directional bimodality in cross-lamination represents intertidal as well as subtidal deposits, whereas the deposition of parallel-laminated sandstone facies under upper flow regime conditions is diagnostic in shallow tidal channels (De Raaf & Boersma, 1971; Terwindt, 1971). The mode of deposition of mud drapes indicates whether the depositional environment is subtidal or intertidal. In the intertidal environment, mud is deposited as only a single layer and in the subtidal environment as mud layer couplets (Visser, 1980). Herringbone structure in cross-laminated/cross-bedded sandstone is a diagnostic feature in tidal environments and trough cross-bedded sandstone facies indicates shallow subtidal environment under the influence of high tidal energy (Alam, 1995).

The fining upward cycle (bell shape) with more than 3 m corresponds to the mesotidal range and indicates intertidal sediment transport processes (Alam, 1995; Terwindt, 1971) and represents retreating shoreline–shelf system in shallow marine setting, fluvial or deltaic channels (Emery & Myers, 1996; Selley, 1985, 1998). The coarsening upward cycle (funnel shape) indicates delta progradation. A coarsening upward cycle overlain by a fining upward cycle (bow shape) indicates tide-dominated delta (mixed tidal flat) and an irregular cycle represents tide-dominated delta (muddy tidal flat). Analysis of sedimentological data from the subsurface Neogene succession in the Sylhet Trough of the Bengal Basin has shown similar tidal signatures, as reported by

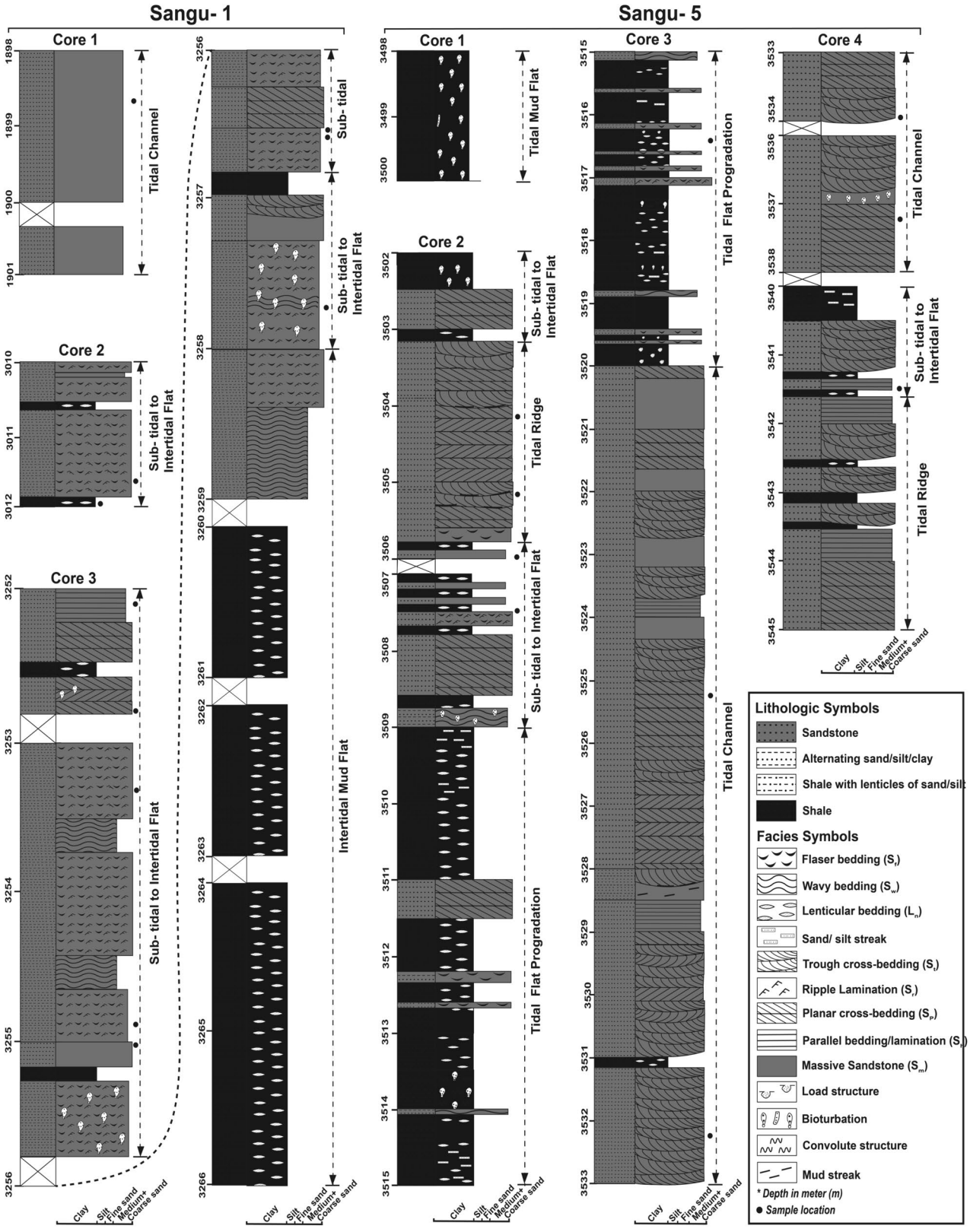

Fig. 7 Detailed core lithologs delineating lithofacies and facies associations and reconstructions of depositional environments of the Neogene sediments, Sangu-1 and Sangu-5 wells (modified after Rahman et al., 2022)

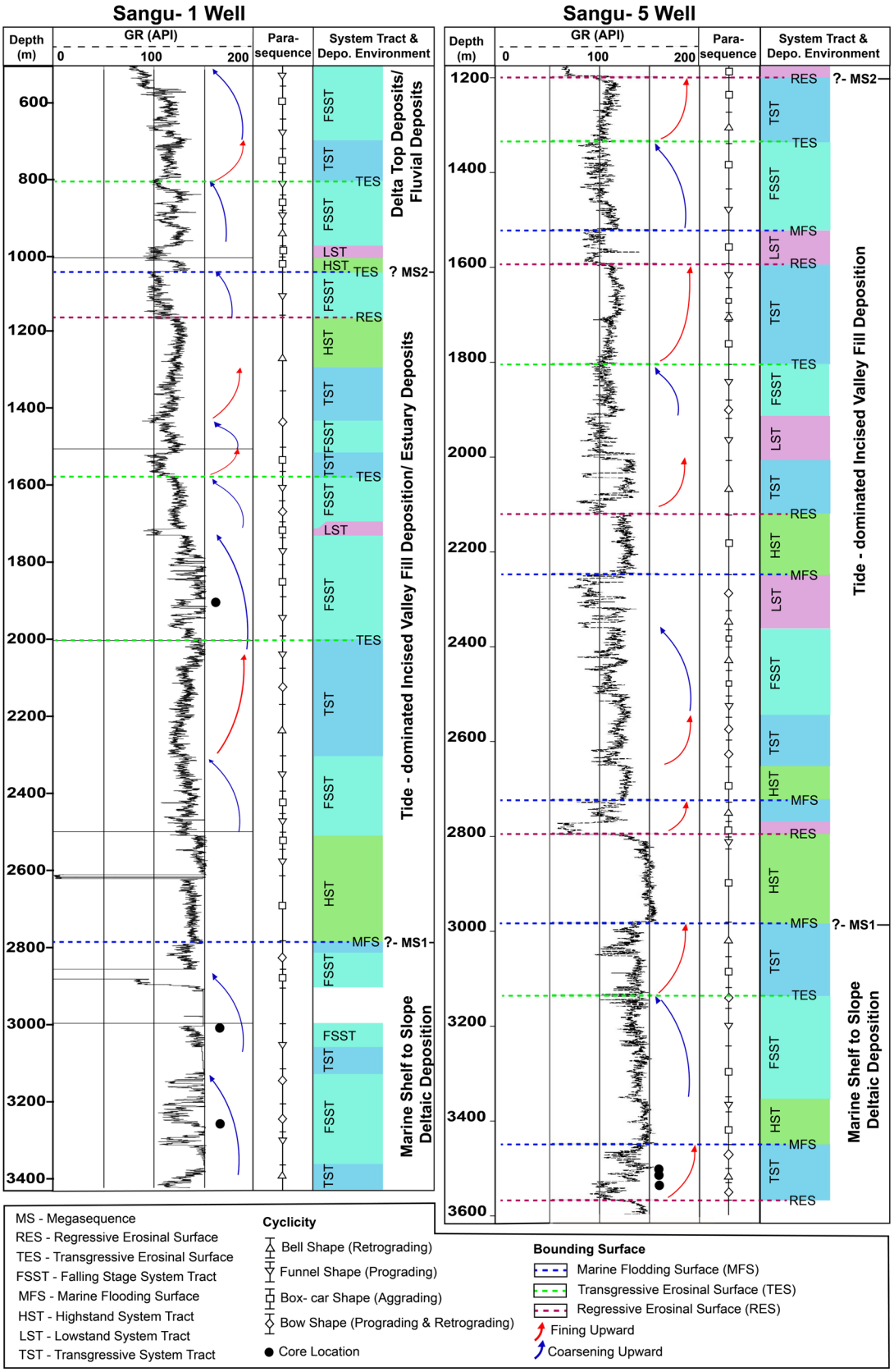

Fig. 8 Parasequences and system tracts are delineated based on gamma ray log response with different bounding surfaces to interpret depositional environments in the Sangu-1 and Sangu-5 wells

Rahman et al. (2009). Additionally, Alam (1995) identified tide-generated structures in the Baraichari Shale Formation, such as herringbone cross-bedding, bundle structure, mud couplet, bipolar cross-lamination with reactivation surfaces, and 'tidal' bedding. The repetitive presence of incised channel, tidal inlet, tidal ridge/shoal, tidal flat, and other tidal deposits, interspersed with shelfal mudstone, has been observed in the southeastern part of the Bengal Basin, as documented by Gani and Alam (2003).

Sequences have been discerned based on gamma ray log responses (Figs. 6, 8) in the Sangu-1 and 5 wells. Depositional sequences have been inferred as highstand system tract (HST), lowstand system tract (LST), falling stage system tract (FSST), and transgressive system tract (TST) (Fig. 8). Boundaries of megasequence-1, megasequence-2, and megasequence-3 (Fig. 9) are approximated from marine flooding surface (MFS), transgressive erosional surface (TES), and regressive erosional surface (RES) (Najman et al., 2012).

Megasequence-1 is the oldest unit and was deposited during the Miocene to Early Pliocene time. The top of megasequence-1 is followed by a maximum marine flooding surface (MFS) representing forestepping, progradational sequence stack. The lithology of these sequence intervals is shale, sandstone/shale alteration, and sandstone with shale thin layers, and stacking patterns indicate an overall coarsening upward sequence deposited in marine delta shelf to slope depositional environment (Najman et al., 2012).

A major and abrupt change in depositional environment results from a basinward shift in facies that is marine regression in megasequence-2. The top of megasequence-2 is followed by a transgressive erosional surface (TES). Aggradational geometries dominate due to an increase in sediment supply in the basin from Paleo-Ganges during the Mid-Miocene time (Cairn Energy, 1998). The repeated cut and fill indicates relative sea-level fluctuations during the deposition of sediments and indicates tide-dominated incised valley-fill deposits. During the Late Pliocene to Pleistocene period, sedimentation and accommodation are generally in equilibrium and the nature of the shelf–slope break is predominantly aggradational (Najman et al., 2012)

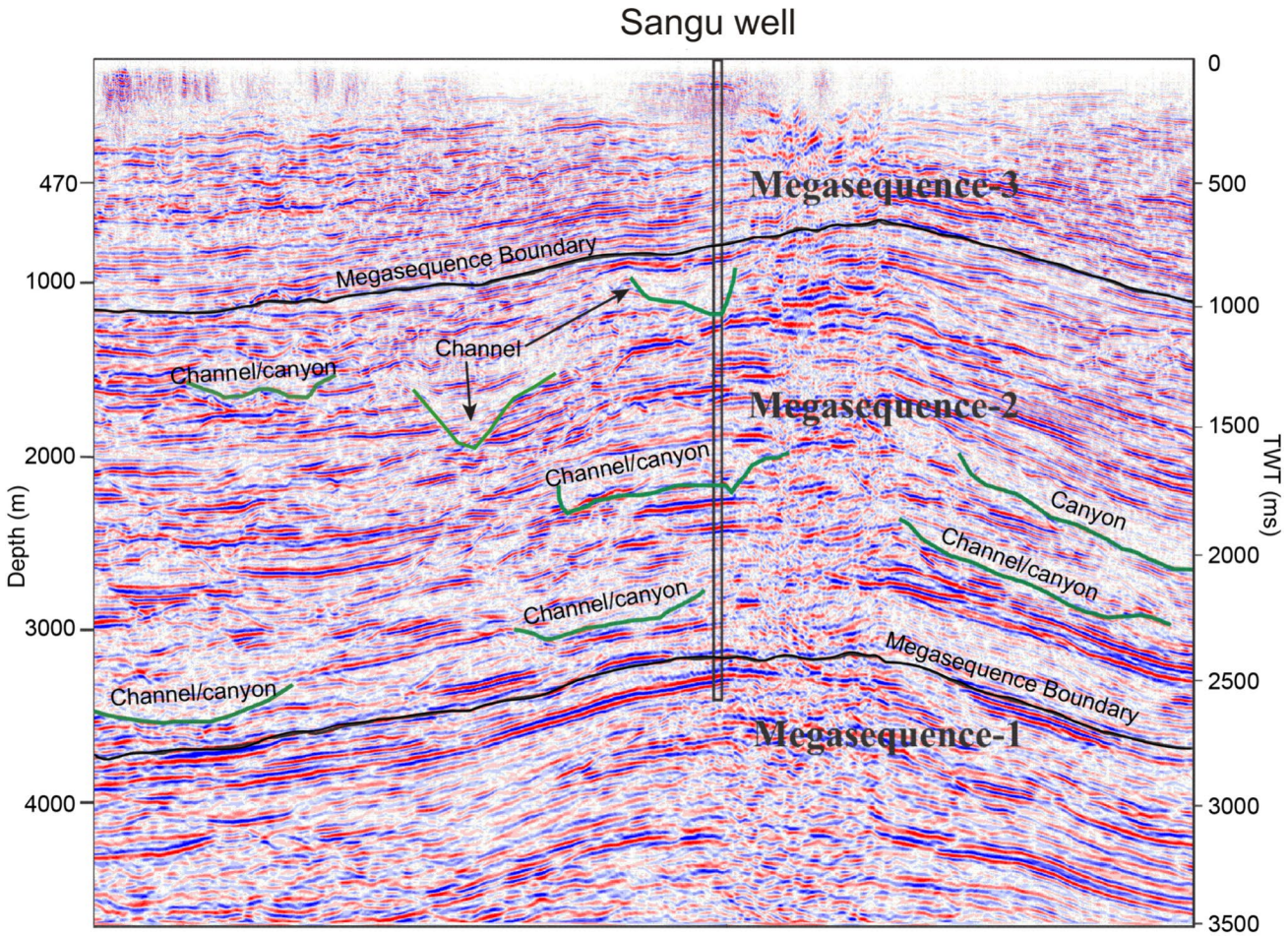

Fig. 9 Seismic megasequences of the Sangu area on the seismic section along line ceb-94-43 with channels and canyons

representing a delta top (fluvial-braided) depositional condition in megasequence-3.

6 Conclusions

1) Seven facies have been recognized distinctively based on texture, lithologic association, and internal sedimentary structures from the core samples of Surma Group encountered in Sangu-1 and Sangu-5 wells such as shale (F_m) and shale with lenticules of sand (lenticular bedded facies, L_n), wavy bedded sandstone facies (S_w), flaser bedded sandstone (S_f) with ripple laminated (S_r) sandstone facies, parallel-laminated sandstone facies (S_h), trough cross-bedded sandstone facies (S_t), planar cross-bedded sandstone facies (S_P), and massive sandstone (S_m) facies. These lithofacies are ramified into three distinct facies associations: shale-dominated facies assemblages, alternating sandstone and shale facies, and sandstone-dominating facies.
2) The presence of lenticular, wavy, flaser bedding, ripple cross-stratification, laminated sand/silt-streaked shales, cross-bedded sandstone with mud drapes, and herringbone cross-stratification indicates strong tidal current evidence and fluctuation of relative sea-level changes had occurred that characterized by repetitive transgressive and regressive phases.
3) In the Sangu-1 (500–3420 m) and the Sangu-5 wells (1175–3660 m depth), five log facies are discerned, namely funnel-shaped facies, bell-shaped facies, boxcar facies, bow-shaped facies, and serrated-shaped facies. Bell-shaped facies indicates intertidal sediment in shallow marine settings, fluvial or deltaic channels, and funnel-shaped facies indicates delta progradation. Bow-shaped facies indicates tide-dominated delta (mixed tidal flat) and serrated-shaped facies represents tide-dominated delta (muddy tidal flat).
4) Interpretation of subsurface seismic profile of line ceb-94 trending SE–NW through the offshore Sangu structure represents that the top of megasequence-1 is followed by a maximum marine flooding surface (MFS) representing forestepping, progradational sequence stack, and the top of megasequence-2 is followed by a transgressive erosional surface (TES) followed by the gradual establishment of the overlying continental–fluvial depositional systems (i.e., the megasequence-3).
5) Finally, it can be adjudged from the above discussion that the paleo-depositional environment of the Neogene Surma Group of the Sangu structure is tide-dominated deltaic. Overall, the understanding of the depositional facies of the Neogene sequences in the offshore regions of the Bengal Basin will play a crucial role in the exploration of hydrocarbons in the untapped areas of the Bay of Bengal.

Acknowledgements This research work was financially supported by the Bangladesh Bureau of Educational Information and Statistics (BANBEIS), Government of the People's Republic of Bangladesh, Ministry of Education (PS2016186). We are grateful to Petrobangla (Bangladesh Oil, Gas and Mineral Corporation) for providing core samples and data support.

Author Contribution 1*-reviewed the manuscript 1-writing manuscript, prepared Figures 2-writing manuscript.

Data availability No datasets were generated or analysed during the current study.

Declaration

Conflict of interest The authors declare no competing interests.

References

Alam, M. M. (1995). Tide-dominated sedimentation in the upper Tertiary succession of the Sitapahar anticline, Bangladesh. *International Association of Sedimentologists Special Paper, 24*, 329–341.

Bakhtine, M. I. (1966). Major tectonic features of Pakistan: Part II. *The Eastern Province. Science & Industry, 4*, 89–100.

Energy, C. (1998). Sangu field evaluation report (Geology and Geophysics). *Edinburgh, 1*, 2–6.

Cant, D. J. (1992). Subsurface facies analysis. In R. G. Walker & N. P. James (Eds.), *Facies models: Response to sea level change. Geological Association of Canada* (pp. 27–45). Newfoundland: St. John's.

Curray, J. R. (1991). Geological history of the Bengal geosyncline. *Journal of Association of Exploration Geophysicists, XII*, 209–219.

Curray, J. R. (2014). The Bengal depositional system: From rift to orogeny. *Marine Geology, 352*, 59–69.

Curray, J. R., Emmel, F. J., & Moore, D. G. (1993). The Bengal fan: Morphology, geometry, stratigraphy, history and processes. *Marine and Petroleum Geology, 19*, 1191–1223.

Curray, J. R., & Munasinghe, T. (1991). Origin of the Rajmahal Traps and the 85°E Ridge preliminary reconstructions of the trace of the Crozet hotspot. *Geology, 19*, 1237–1240.

De Raaf, J. E. M., & Boersma, J. R. (1971). Tidal deposits and their sedimentary structures. *Geologie En Mijnbouw, 50*(4), 79–503.

Emery, D., & Myers, K. J. (1996). *Sequence Stratigraphy*. Blackwell Science.

Gani, M. R., & Alam, M. M. (2003). Sedimentation and basin-fill history of the Neogene clastic succession exposed in the southeastern fold belt of the Bengal Basin, Bangladesh: A high-resolution sequence stratigraphic approach. *Sedimentary Geology, 155*, 227–270.

Ginsburg, R. N. (1975). *Tidal deposits*. Springer-Verlag.

Greve, J., Busch, B., Quandt, D., Knaak, M., & Hilgers, C. (2024). The influence of sedimentary facies, mineralogy, and diagenesis on reservoir properties of the coal-bearing Upper Carboniferous of NW Germany. *Journal of Petroleum Geoscience*. https://doi.org/10.1144/petgeo2023-020

Guha, D. K. (1978). Tectonic framework and oil & gas prospects of Bangladesh. In *Proceedings of the 4th Annual Conference Bangladesh Geological Society*, pp. 65–75.

Hossain, M. S., Khan, M. S. H., Chowdhury, K. R., & Abdullah, R. (2019). Synthesis of the tectonic and structural elements of the Bengal Basin and its surroundings. In S. Mukherjee (Ed.), *Tectonics and structural geology: Indian context* (pp. 135–218). Cham: Springer International Publishing AG.

Hossain, M. S., Xiao, W., Khan, M. S. H., Chowdhury, K. R., & Ao, S. (2020). Geodynamic model and tectono-structural framework of the Bengal Basin and its surroundings. *Journal of Mapsm, 16*(2), 445–458.

Irfan, M., Singh, B. P., & Kanhaiya, S. (2022). Textural behaviour, facies, and depositional environments of the Middle Siwalik Subgroup of the Jammu area, Jammu & Kashmir State, NW Himalaya. *Journal of the Paleontological Society of India, 67*(1), 85–92.

Kanhaiya, S., Singh, B. P., Tripathi, M., Sahu, S., & Tiwari, V. (2017). Lithofacies and particle-size characteristics of late Quaternary floodplain deposits along the middle reaches of the Ganga River, Central Ganga Plain, India. *Geomorphology, 284*, 220–228.

Khanam, S., Khan, K. F., Quasim, M. A., Kanhaiya, S., & Ahmad, F. (2022). Proterozoic sandstone of Rajgarh Formation, Alwar sub-basin, North-eastern Rajasthan: Sedimentological and paleohydrodynamical implications. *Journal of Sedimentary Environments., 7*(3–4), 1–22.

Klein, G. D. V. (1971). A sedimentary model for determining paleotidal range. *Geological Society of America Bulletin, 82*, 2585–2592.

Klein, G. D. V. (1985). Intertidal flats and intertidal sand bodies. In R. A. J. Davis (Ed.), *Coastal sedimentary environments* (pp. 185–224). Springer-Verlag.

Krassay, A. A. (1998). Outcrop and drill core gamma ray logging integrated with sequence stratigraphy: Examples from Proterozoic sedimentary successions of northern Australia. *AGSO Journal of Australian Geology and Geophysics, 17*(4), 285–299.

Miall, A. D. (2010). *The geology of stratigraphic sequences*. Springer.

Matesic, M. (2012). *Depositional Environment, Thin Bed Potential, Evaluation Strategy at Offshore Fields, Bay of Bengal, Bangladesh* (pp. 16–19). Singapore: American Association of Petroleum Geologists International Convention and Exhibition.

Matin, M. A., Fariduddin, M., Husain, M. T., Khan M. M., Boul, M. A., & Kononov, A. I. (1986). New concepts on the tectonic zonation of Bengal foredeep. In *Offshore South-east Asia Conference*, Singapore.

Maurin, T., & Rangin, C. (2009). Structure and kinematics of the Indo-Burmese Wedge: Recent and fast growth of the outer wedge. *Tectonics, 28*, TC2010. https://doi.org/10.1029/2008TC002276

Najman, Y., Allen, R., Willett, E. A. F., Carter, A., Barford, D., Garzanti, E., Wijbrans, J., Bickle, M., Vezzoli, G., Ando, S., Oliver, G., & Uddin, M. (2012). The record of Himalayan erosion preserved in the sedimentary rocks of the HatiaTrough of the Bengal Basin and the Chittagong Hill Tracts, Bangladesh. *Basin Research, 24*, 1–21.

Najman, Y., Sobel, E.R., Millar, I., Luan, X., Zapata, S., Garzanti, E., Parra, M., Vezzoli, G., Zhang, P., Wa Aung, D., Paw, S. M. T. L., & Lwin, T. N. (2022). The timing of collision between Asia and the West Burma Terrane, and the development of the Indo-Burman Ranges; *Tectonics, 41*(7). https://doi.org/10.1029/2021TC007057

Najman, Y., Bracciali, L., Parrish, R. R., Chisty, E., & Copley, A. (2016). Evolving strain partitioning in the Eastern Himalaya: The growth of the Shillong Plateau. *Earth and Planetary Science Letters, 433*, 1–9.

Petrobangla. (2016). *Bangladesh Acreage Block Map*. Bangladesh Transverse Mercator.

Rahman, M. J. J., Faupl, P., & Alam, M. M. (2009). Depositional facies of the subsurface Neogene Surma Group in the Sylhet Trough of the Bengal Basin, Bangladesh: Record of tidal sedimentation. *International Journal of Earth Sciences, 98*(8), 1971–1980.

Rahman, M. J. J., Xiao, W., Hossain, M. S., Yeasmin, R., Sayem, A. S. M., Ao, S., Yang, L., Abdullah, R., & Dina, N. T. (2020). Geochemistry and detrital zircon U-Pb dating of Pliocene-Pleistocene sandstones of the Chittagong Tripura Fold Belt (Bangladesh): Implications for provenance. *Gondwana Research, 78*, 278–290.

Rahman, M. J. J., Xiao, W., McCann, T., & Ao, S. (2017). Provenance of the Neogene Surma Group from the Chittagong Tripura Fold Belt, southeast Bengal Basin, Bangladesh: Constraints from whole-rock geochemistry and detrital zircon U-Pb ages. *Journal of Asian Earth Sciences, 148*, 277–293.

Rahman, M. J. J., Mutti, M., Ma, M., Chen, G., Akhter, W., Akter, S., Hossain, M. S., & Khan, M. R. A. (2022). Diagenetic controls on the reservoir quality of Neogene sandstones in the offshore area of the Bengal Basin, Bangladesh. *Geological Journal, 57*, 4793–4814.

Reimann, K. U. (1993). *Geology of Bangladesh*. Berlin: Gebruder Borntraeger.

Reineck, H. E., & Singh, I. B. (1980). *Depositional sedimentary environments* (4th ed.). Springer-Verlag.

Reineck, H. E., & Wunderlich, F. (1968). Classification and origin of flaser and lenticular bedding. *Sedimentology, 11*, 99–104.

Shahriar, M. U., Hossain, D., Hossain, M. S., Rahman, M. J. J., & Kamruzzaman. (2020). Geophysical characterization of the Sangu Gas Field, Offshore, Bangladesh: Constraints on reservoirs. *Journal of Petroleum Geology, 43*(4), 363–382.

Shamsuddin, A. H. M., & Abdullah, S. K. M. (1997). Geological evolution of the Bengal Basin and its implication in hydrocarbon exploration in Bangladesh. *Indian Journal of Geology, 69*, 93–121.

Shamsuddin, A. H. M. (2022). Petroleum System of Bangladesh and Its Hydrocarbon Reserves and Resources. In K. R. Chowdhury, M. S. Hossain, & M. S. H. Khan (Eds.), *Bangladesh geosciences and resources potential* (pp. 157–220). Taylor & Francis: CRC Press.

Selley, R. C. (1985). *Elements of petroleum geology*. New York: W. H. Freeman and company.

Selley, R. C. (1998). *Elements of petroleum geology*. Academic Press.

Singh, B. P., & Singh, H. (1995). Evidence of tidal influence in the Murree Group of rocks of the Jammu Himalaya, India. *International Association of Sedimentologists Special Paper, 24*, 343–351.

Singh, B. P., Mondal, K., Singh, A., Mittal, P., Singh, R. K., & Kanhaiya, S. (2020). Seismic origin of the soft-sediment deformation structures in the upper Palaeo-Mesoproterozoic Semri Group, Vindhyan Supergroup, Central India. *Geological Journal, 55*(11), 7474–7488.

Singh, A., Bhushan, K., Singh, C., Steckler, M. S., Akhter, S. H., Seeber, L., Kim, W.-Y., Tiwari, A. K., & Biswas, R. (2016). Crustal structure and tectonics of Bangladesh: New constraints from inversion of receiver functions. *Tectonophysics, 680*, 99–112.

Terwindt, J. H. J. (1971). Lithofacies of inshore estuarine and tidal inlet deposits. *Geologie En Mijnbouw, 50*, 515–526.

Uddin, A., & Lundberg, N. (1998). Cenozoic history of the Himalayan-Bengal system: Sand composition in the Bengal basin, Bangladesh. *Geological Society of American Bulletin, 110*, 497–511.

Visser, M. J. (1980). Neap-spring cycles reflected in Holocene subtidal large-scale bedform deposits: A preliminary note. *Geology, 8*, 543–546.

Yadav, S. K., Kanhaiya, S., Singh, S., Quasim, M. A., Singh, S. K., & Kumar, P. (2023). Facies dispersal patterns and textural attributes of the Late Quaternary floodplain sediments of the Sai River, Central Ganga Plain, India. *Geosystems and Geoenvironment, 2*(1), 100216.

Yang, L., Xiao, W., Rahman, M. J. J., Windley, B. F., Schulmann, K., Ao, S., Zhang, J., Chen, Z., Hossain, M. S., & Dong, Y. (2020). Indo-Burma passive amalgamation along Kaladan Fault: Insights

from provenance of Chittagong-Tripura Fold Belt (Bangladesh). *Geological Society of America Bulletin, 132*(9–10), 1953–1968.

Yang, L., Xiao, W., Rahman, M. J. J., Windley, B. F., Schulmann, K., Ao, S., Chen, Z., & Li, R. (2019). Provenance of the Cenozoic Bengal Basin sediments: Insights from U-Pb ages and Hf isotopes of detrital zircons. *Geological Journal, 54*, 978–990.